Proceedings of the 21st ICSMGE, Vienna, Austria, 14 – 19 June 2026. Pistrol, Adam & Schweiger (eds.)
Published by: ÖGG, Austrian Society for Geomechanics, Salzburg, Austria, ISBN 978-3-9503898-4-5
https://doi.org/10.53243/ICSMGE2026-2134

Impact of Soil Water Characteristics of Unsaturated Soil on Corrosion of Metal/Alloys

Waqas Akhtar, Gemmina Diemidio, Wim Cornelis
University Ghent Geotechnical Institute, Ghent University, Belgium, Waqas.akhtar@ugent.be
University Ghent Geotechnical Institute, Ghent University, Belgium, Gemmina.Diemidio@ugent.be
Department of Environment, Ghent University, Belgium, Wim.Cornelis@UGent.be

ABSTRACT: Corrosion in buried infrastructure is the main concern, underground pipelines, foundations of solar panels, and steel structures are prone to corrosion. Almost one-third of the damage is caused by corrosion. Soil moisture has been identified as major influencing factors governing corrosion in soils. This study aims to investigate the optimal moisture content of different percentages of kaolinite clay mixed sand and to determine the air-water phase called Air Transition Point (ATP) using soil water characteristics curves (SWCCs) from two commonly known methods. The filter paper as per ASTM D-5298 method widely used in geotechnics and newly modified evaporation method known as Hydraulic Property Analyzer (Hyprop). The fine structure of kaolinite clay and its ability to retain moisture having less plasticity and less prone to swelling contribute to the corrosion, due to trapping moisture and oxygen near steel surface. As the percentage of fines increases, the ATP shifts more towards the right in the suction graphs. The steel coupons were placed in the kaolinite-sand mixture upon optimal moisture content the result of weight loss test and the morphology of fine content and steel was extracted.

KEYWORDS: Air Transition Point (ATP), Fine Content, Weight Loss, Corrosion rate.

1 INTRODUCTION

Corrosion poses a critical threat to buried infrastructure including underground pipelines, foundations for solar panels, and subterranean steel elements is a prevalent issue, with soil induced corrosion. The soil moisture parameters are key to understanding corrosion behavior, as it directly influences soil resistivity, oxygen diffusion, and electrolyte conduction at the metal-interface, while the soil moisture has been repeatedly identified as a primary governing variable. The soil water retention curve (SWRC) describes the relationship between volumetric water content (θ) and matric suction (ψ), which is central to understanding unsaturated soil hydraulics. Under low suction (near saturation), capillary forces dominate at high suction, adsorption. (Azoor et al., 2022; van Genuchten, 1980). Consequently, the degree of saturation within the soil matrix surrounding a buried structure profoundly impacts the corrosion rate. However, the relationship is complex and non-linear. Very low moisture levels can drastically reduce corrosion rates by limiting ionic mobility and oxygen diffusion of oxygen, the primary cathodic reactant in near neutral soils. The critical zone for maximum corrosion susceptibility often lies in the intermediate moisture range, where sufficient electrolyte is present for ionic conduction, yet sufficient air-filled pore exits to supply oxygen to the metal surface (Cole & Marney, 2012).(Miyauchi et al., 2025) Moisture acts as an electrolyte, enabling ionic flow between anodic and cathodic sites on metal surfaces. However, the relationship is nonlinear. Corrosion peaks in the intermediate moisture range where oxygen diffusion and ionic conductivity are optimized, this zone, termed as Air Transition Point (ATP) represents a critical threshold in the soil's pore structure (Fredlund et al., 2011; Rahardjo et al., n.d.). The fine-grained soils, particularly kaolinite clay, exacerbate corrosion risk due to their unique microstructure. Kaolinite ($Al_2Si_2O_5(OH)_4$) possesses high specific surface area and layered morphology, enabling significant moisture retention even at low plasticity indices, unlike expansive smectite clays, kaolinite exhibits limited swelling, forming stable micro-pores that trap moisture and oxygen near steel interfaces (Castro, Park, Sherik, et al., 2025; James K. Mitchell, 2005) . When mixed with coarser materials like sand common in backfills and subgrades the resulting pore size distribution dictates hydraulic behavior. As kaolinite content rises, the soil water retention capacity increases, shifting the ATP towards higher suction value (Leong & Rahardjo, 1997). The SWRC is essential for characterizing ATP, as it describes suction moisture relationships across saturation states. Traditional methods like filter paper techniques (ASTM D 5298) measure suction directly and indirectly via moisture equilibrium. However, it takes long equilibrium time and is sensitive to operator technique (Khan et al., 2022; Shwan, 2024). The evaporation method is now becoming popular in soil science known as Hydraulic Property Analyzer (Hyprop) is a laboratory instrument used to determine hydraulic properties of soils using two precision mini-tensiometers capturing high resolution SWCC data for suction $\leq$ 100 kPa (Rajkai et al., 2004; Ridley & Borland, 1993; Shokrana & Ghane, 2020; van Genuchten, 1980). Moreover, many researchers found degree of saturation is the dominant control on corrosion, overshadowing pore fluid conductivity, maximum corrosion occurs at intermediate saturation (≈50–80%), where continuous air and water pathways enable efficient electrochemical cells. However, the corrosion mechanism and chemical transport are also fundamentally dependent on pore fluid pH, furthermore, local heterogeneity in packing and moisture distribution strongly influences localized corrosion rate, the corrosion behavior of mild steel buried in clay soils under varying moisture content and compaction levels has maximum corrosion mass loss and pitting depth consistently occurred at a soil moisture content of 17-18%w, while increased compaction had minimal effect on corrosion in finely graded clays, poorly compacted lumpy clays exhibited greater localized corrosion and deeper pits due to larger air voids between steel and soil interface, over time the corrosion progressed from localized to pitting more uniform pattern. (Castro, Park, Cha, et al., 2025; Petersen & Melchers, 2019). Despite this understanding, quantitative links between kaolinite-sand composition, ATP, and corrosion rates remain poorly defined. This study bridges these gaps by investigating how kaolinite content in sand mixtures alters SWRCs derived from ATPs and corrosion behavior.

2 MATERIALS AND EXPERIMENTAL METHODSTITLE OF

The kaolinite clay used in this study, Polwhite B China Clay from Imerys Kaolinite Company, is a premium, medium-sized particle material obtained from a deposit in Southwest England.

The kaolinite was combined with silica sand in five different proportions (10%, 15%, 20%, 25%, and 30% KC by weight). The corresponding material properties are provided in Table 1. The optimum moisture content was determined in accordance with ASTM 698, while the soil-water retention properties were assessed using both filter paper method and the Hyprop method. Whatman 42 ashless filter paper was used following ASTM D 5298-03. The grain size distribution of kaolinite clay and silica sand are presented in Figure 1. And the resulting data was modeled using the van Genuchten-Mualem (VG) equation (Van Genucthen 1980) as shown in Equation 1.

Table 1. Physico-chemical properties of KC.

Parameter	Value
Brightness ISO	82.5±10
Moisture (%)	1.5
pH	5.4
Specific Gravity	2.609
Water Soluble Salt content (%)	0.15
Oil Absorption (g/100g)	38
SiO_2 (%)	47
Al_2O_3 (%)	37
Liquid limit (%)	63
Plastic limit (%)	38
Plasticity index (%)	24

$$\theta=\theta_r+\frac{\theta_s+\theta_r}{[1+(\alpha|h|)^n]^m} \quad (1)$$

Where θ is the water content ($L^3\ L^{-3}$), θr and θs are residual and saturated water content, α is the inverse of air entry value (L^{-1}), n and m are the curve fitting parameters, where m=1-1/n. The grain size distribution curve of kaolinite sand mixture is shown in Figure 1. The air entry value (AEV), described as the pressure head at which air initially starts to replace water in the largest soil pores, was determined by Van Genuchten model parameters α (AEV ≈ 1/α) [1]. For the electrochemical characterization the steel coupons (60mm*60mm*0.5mm) specimen was used. To ensure surface uniformity, the steel coupons were sequentially polished using sandpapers with grit sizes of 80, 240, 350, 400, 600, 800, 1000, and 1200. Following polishing, all coupons were thoroughly cleaned in an ultrasonic bath using acetone and ethanol to eliminate any surface contaminants and then air-dried. The specimens were subsequently embedded in kaolinite–silica sand mixtures containing varying kaolinite contents (10%, 15%, 20%, 25%, and 30% by dry weight of silica sand) and compacted to their respective optimum moisture contents in accordance with ASTM D698. For accuracy and reliability of the results, each mixture contained two steel coupon specimens placed horizontally within the mixture.

The Steel corrosion experiments were conducted using kaolinite–silica sand mixtures with varying kaolinite contents (10%, 15%, 20%, 25%, and 30% by dry weight of silica sand). For each mixture, two steel coupon specimens were placed horizontally within the compacted soil at their respective optimum moisture content (as determined by ASTM D698).

The prepared samples were placed in a sealed bucket and stored under controlled laboratory conditions. This controlled environment minimized thermal variability and ensured repeatability of experimental results. The specimens were left undisturbed for two exposure periods: 45 days and 95 days to allow corrosion to develop under controlled conditions.

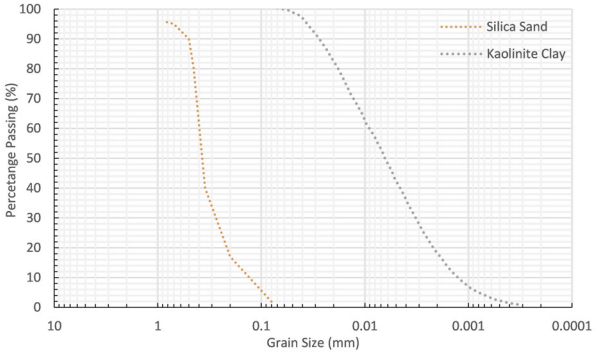

Figure 1. Kaolinite clay and silica sand distribution curve.

At the end of each exposure period, the steel coupons were carefully extracted from the soil mixtures. The coupons were then cleaned to remove adhered soil and corrosion products using acetone and soft brushing, followed by air-drying. The cleaned specimens were weighed using a high-precision digital balance to determine the mass loss due to corrosion. To systematically evaluate the corrosion damage, surface morphology analysis was performed using scanning electron microscopy (SEM) and Energy-dispersive spectroscopy (EDS) were subsequently conducted to quantify elemental distributions, with particular attention to iron oxidation products and potential clay-mineral interactions at the interface. This combined microstructural and compositional analysis revealed the corrosion mechanisms specific to the kaolinite-sand in controlled Laboratory environment. The specimens were first gently brushed to remove the soil particles and were
were cleaned with ethanol to remove corrosion residues. After drying, they were immediately weighed using 4-digit analytical balance to determine the mass loss, the chemical properties were shown in Table2.

Table 2. Chemical Properties of Metal/Alloys.

Chemical Properties	Value (wt%)
C	0.025
P	0.03
S	0.02
Mn	0.25
Cr	17.58
Si	0.4
Ni	10.09
Fe	Bal

The weight loss (WL) was calculated using $WL=W_i-W$
Where W_i is initial weight of the steel coupons (g)
W_f is final weight of steel coupons (g)
The Corrosion rate (CR) μm/year is determined by using equation 2.

$$CR=+\frac{87{,}600\Delta W}{A.T.D} \quad (2)$$

Where: W= Weight loss (g)
A= Surface area of coupon (cm^2)
T= Exposure time (hours)
D= Density of steel (g/cm^3)

The measured weight loss and calculated corrosion rates were then used to quantitatively evaluate the effect of kaolinite content and exposure duration on steel degradation.

3 RESULTS AND DISCUSSION

The SWRCs of kaolinite–silica sand mixtures (10–30% KC) obtained via FP and Hyprop methods showed consistent results. Increasing kaolinite content led to systematic changes in hydraulic properties shown in Figure 2. The measured air entry value (AEV) progressively increases from 1.731, 8.660,

17.886, 26.41, and 36.184 kPa in the boundary zone. The air transition point, where moisture retention shifts from capillary to adsorption, showed moisture content rising from 6.22% to 13.62%, moving toward the residual zone. These moisture shifts promote corrosion in steel, influenced by soil type. Furthermore, the results, as presented in Figure 3, demonstrate that steel specimens embedded in soil with 10% kaolinite content (KC) experienced a higher corrosion rate compared to those in 15%, 20%, 25%, and 30% KC. It indicates that while kaolinite content increases the corrosion resistance of the soil-steel system. The improvement may be attributed to the finer particle size and higher retention. The micromorphology and element content of corrosion product is evaluated by using Scanning Electron Microscopy equipped with Energy Dispersive X-ray analysis. The corrosion products formed small, densely packed agglomerates on the specimen, without significant voids.

The EDS analysis revealed that the formed corrosion residues predominantly consisted of ferrous (Fe), oxygen (O), and Silicon (Si). The reddish-brown corrosion products observed on the specimen strongly suggesting the formation of ferric oxide (Fe_2O_3), as the dominant phase. Which is consistent with the characteristic coloration of this oxide. The presence of Si in the corrosion layer indicates incorporation from the 10% kaolinite clay ($Al_2Si_2O_5(OH)_4$) and 90% silica sand (SiO_2) mixture elucidated the specific role of the clay-sand mixture in the corrosion mechanism.

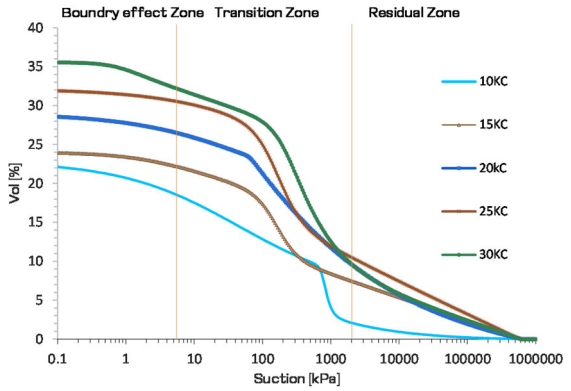

Figure 2. SWRC of kaolinite clay mixtures.

These changes in moisture significantly influence the corrosion behavior of embedded steel, depending on the soil composition. As shown in Figure 3, steel specimens embedded in the soil with 10% kaolinite content exhibited higher corrosion rates compared to those in soils containing 15%, 20%, 25%, and 30% KC. This suggests that increasing kaolinite content enhances the corrosion resistance of the soil–steel system, likely due to the finer particle size and greater moisture retention of the clay, which limits oxygen and electrolyte mobility at the metal interfaces. Figure 3(a) shows the corrosion rate measurements of metal coupons embedded in kaolin-sand soil mixtures after 45 days of exposure under varying moisture levels (expressed as a percentage of the crop coefficient, %KC). The corrosion rate trends indicate a relatively lower rate across all moisture levels. However, even at this early exposure period, distinct variations can be observed. At lower moisture content (10% KC), corrosion rates are slightly elevated but remain below 2 µm/year. As the moisture increases up to 30% KC, a more fluctuating pattern appears, reflecting localized electrochemical activity likely due to pore water availability and oxygen diffusion differences.

The presence of low and sporadic peaks signifies the onset of corrosion but not yet at its full intensity.

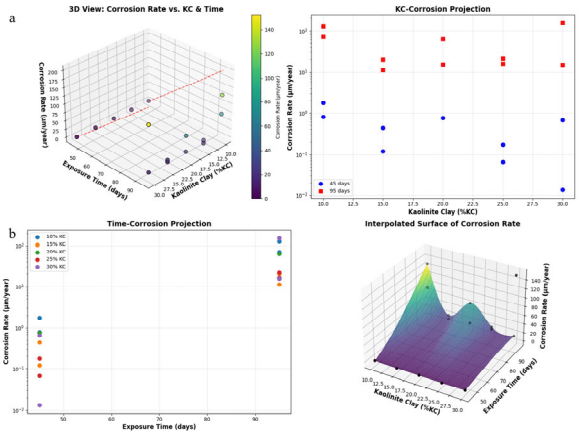

Figure 3. Effect of kaolinite clay on corrosion rate.

In contrast, Figure 3(b) illustrates the corrosion rate after 95 days of exposure under the same moisture conditions. A significant increase in corrosion activity is evident at certain points (notably at 10% KC and 30% KC). This substantial jump suggests that prolonged exposure in moist environments exacerbates electrochemical degradation, especially when the soil is either too dry to resist ionic migration or too saturated to limit oxygen. Interestingly, mid-range moisture levels (15–25% KC) show relatively lower corrosion peaks, hinting at a possible Air Entry Value (AEV) influence where the corrosion conditions are temporarily buffered.

4 CONCLUSIONS

This study systematically correlates kaolinite clay content (10-30% KC) in silica sand mixtures with evolving hydraulic properties and corrosion behaviour. SWRC analysis revealed a direct relationship between KC content and hydraulic parameters such as air entry values increased from 1.731 kPa (10% KC) to 36.184 kPa (30% KC), while the transition from capillary to adsorption-dominated moisture retention shifted from 6.22% to 13.62% water content. These hydraulic transitions create distinct electrochemical environments, with 10% KC mixtures exhibiting the most aggressive corrosion conditions. The results clearly demonstrate that both moisture content and exposure duration significantly influence the corrosion behavior of metal in soil environments. After 45 days, corrosion activity remains minimal and somewhat irregular, suggesting early-stage reactions. However, by 95 days, corrosion intensifies drastically, particularly at extreme ends of the moisture scale—both low and high. This suggests that there exists a transitional moisture threshold (likely associated with the Air Transition Point) where corrosion conditions become optimal. The interpolated surface plot confirms this nonlinear relationship, highlighting the need for precise moisture control in geotechnical designs involving buried metallic elements to mitigate long-term corrosion risks.

5 ACKNOWLEDGEMENTS

The Author would like to Acknowledge the financial support provided by Higher Education Commission of Pakistan under (AHPB) Batch IV program and CWO Ghent University for mobility fund. The author would like to sincerely thanks Mr. Filip Van Boxstael, Mr. Maarten Volckaert, Mr. Pol Gryson, and Mr. Asif Ali for their expertise and valuable technical assistance and support during the laboratory work.

6 REFERENCES

Azoor, R. M., Deo, R. N., Birbilis, N., & Kodikara, J. (2019). On the optimum soil moisture for underground corrosion in different soil types. *Corrosion Science*, 159. https://doi.org/10.1016/j.corsci.2019.108116.

Castro., M. G., Park., J. Cha., W. Sherik., A. Santamarina., J. (2025). Metal corrosion in partially saturated sands: pore fluid conductivity and water saturation., *Canadian Geotech journal, 62:1-13* https://doi.org/10.1139/cgj-2024-0097

Castro., M. G., Park., J. Cha., W. Sherik., A. Santamarina., J. (2025b). Corrosion processes in metal buried in sediments: Effect of Fines content, Mineralogy, and Degree of saturation., *Journal of Geotechnical and Geoenvironmental Engineering.* 151(11) http://doi.org/10.1061/JGGEFK.GTENG-13610.

Collis-George, N. (1967). A filter-paper method for determining the moisture characteristics of soil. *Australian Journal of Experimental Agriculture*, 7(25). https://doi.org/10.1071/EA9670162.

Genuchten., V., M. (1980). A closed form equation of predicting the Hydraulic conductivity of unsaturated soils. *Soil Science Society of American Journal*. 44(5), 882-898.

He, C., Wang, Z., You, Y., Wang, X., Zhao, P., Yang, Z., & Zhou, L. (2025). Influence of soil variability on the corrosion of buried hot-dip galvanized steel. *International Journal of Electrochemical Science, 2*0(1). https://doi.org/10.1016/j.ijoes.2024.100889.

Leong, E., Rahardjo, H. (1997). Review of soil water characteristics curve equations. *Journal of Geotechnical and Geoenvironmental Engineering.* Vol. 123, 1106-1117.

Miyauchi, M., Ooi, A., Tada, E. (2025). Effect of Soil Moisture on Corrosion Behavior of Zinc in Simulated Soil Environment. *Japan Society of corrosion Engineering.* Vol, 66, No. 1, pp. 76-84.

Petersen., R. Melchers., R. (2019). Effect of moisture content and compaction on the corrosion of mild steel buried in clay soils., *Journal of Corrosion Engineering Science and Technology*., 54(7). 587-600. https://doi.org/10.1080/1478422X.2019.1638564

Shwan, B. (2024). Soil-water retention curve, determining sands using filter paper method., *Journal of Geotechnical and Geoenvironmental Engineering*. Vol, 150. http//: 10.1061/jggefk.gteng-11405.

Rahardjo, H. Fredlund, D. (1993). An overview of unsaturated soil. Conference: *ASCE Specialty Session Unsaturated Soil Properties at Dallas Texas*, USA. 24-28.

Rajkai, K., Kabos, S., & Van Genuchten, M. T. (2004). Estimating the water retention curve from soil properties: Comparison of linear, nonlinear and concomitant variable methods. Soil and Tillage Research, 79(2 SPEC.ISS.), 145–152. https://doi.org/10.1016/j.still.2004.07.003.

Ridley, A. M., & Borland, J. B. (1993). A new instrument for the measurement of soil moisture suction. *Geotechnique*, *43*(2), 321–324. https://doi.org/10.1680/geot.1993.43.2.321.

Fredlund, D. G., Gan, J. K. M., & Gallen, P. (n.d.-a). Transportation Research Record No. 1481, *Environmental Moisture Effects on Transportation Facilities and Non-earth Materials' Thermal Effects on Pavements.*

Bicalho, K. V, Gomes Correia, A., Ferreira, S., & Marinho, F. A. M. (n.d.). *Filter paper method of soil suction measurement Método del papel de filtro para la medida de la succión del suelo*.

International, A., & indexed by mero, files. (2010). *Standard Test Method for Measurement of Soil Potential (Suction) Using Filter Paper [1]*.

American Society for Testing and Materials, 2003. ASTM D5298-03 *Standard Test Method for Measurement of Soil Potential (Suction) Using Filter Paper*. West Conshohocken, PA: ASTM.